J. Agric. Sci. Technol. (2007) Vol. 9: 287-303

Land Surface Temperature in the Yardang Region of Lut Desert (Iran) Based on Field Measurements and Landsat Thermal Data

S. K. Alavipanah[1]*, M. Saradjian[2], Gh. R. Savaghebi[3], Ch. B. Komaki[1], E. Moghimi[4] and M. Karimpour Reyhan[1]

ABSTRACT

Due to the hard climatic conditions of the yardang region in the Lut Desert, not much information about land surface temperatures of this region, one of the extremely arid climatic zones of Iran, has been extracted. Therefore, in this study in order to obtain some information about important surface features of the Lut Desert (marl, grey sand, bright sand and salt affected land), field temperature measurements were taken and remotely sensed data processing were made. Temperature was measured eight times from 6 a.m. to 8 p.m. during a 15-day period in October 2000. In addition to field measurements, Land sat satellite TM thermal data dated on the 25th of June, 1989 and other sources of data and maps were used. Thermal remote sensing analysis was applied for mapping surface temperatures in the south-eastern part of the Lut Desert in Iran. In this research, the methodology comprised : 1) field temperature measurements, 2) the relationship between the temperature of different soil surfaces and land cover types, 3) diurnal variations in the surface temperature of land cover types, 4) primary image processing and fieldwork, 5) image processing and calibration,6) image classification and accuracy assessment, and 7) land surface temperature mapping. The results obtained have shown the differences between the surface temperatures of the studied features. The significant differences between surface temperatures were discussed. The results obtained have also shown the importance of thermal sensor selection from the viewpoint of satellite overpass time. The results obtained from thermal data and field temperature measurements have shown the time of Landsat satellite overpass has to be considered for image interpretation. As a result, the temperature lowers, respectively, in regions such as yardangs, desert pavement, salty lands, and wetlands; however, it increases in sandy regions.

Keywords: Image processing, Land surface temperature, Lut Desert, Radiance, Sand dune, TM bands, Yardang.

INTRODUCTION

Land surface temperature (LST) is an important factor controlling most physical, chemical, and biological processes of the Earth. Knowledge of LST is necessary for many environmental studies and management activities of the earth resources (Li and Becker, 1993). This extensive requirement of land surface temperature (LST) for environmental studies and management activities of the earth resources has made thermal remote sensing an important academic topic during the last two decades. Temperature is

1. Department of Cartography, Faculty of Geography, University of Tehran, Tehran, Islamic Republic of Iran.
2. Department of Surveying and Geography, Faculty of Engineering, University of Tehran, Tehran, Islamic Republic of Iran.
3. College of Agriculture, University of Tehran, Karaj, Islamic Republic of Iran.
4. Faculty of Physical Geography Department, University of Tehran, Islamic Republic of Iran.
* Corresponding author, e-mail: salavipa@ut.ac.ir

[DOR: 20.1001.1.16807073.2007.9.4.1.2]

a fundamental thermodynamic quantity used to describe the state of matter and to quantify the transport of heat. Temperature is such an essential factor in understanding all physical, chemical and biological systems on earth and space that Norman *et al*. (1995) stated it must be considered in any studies involving earth sciences.

Thermal remote sensing offers the possibility of monitoring the surface energy budget on regional and global scales (Norman *et al*., 1995). But the limited success associated with the use of thermal remote sensing may arise from: 1) the presence of numerous variables that can affect surface temperature, 2) the difference between thermal properties and surface reflectance, and 3) the difference between spatial resolution of thermal and reflective bands. However, evidence based on environmental studies has shown the practical applications of thermal remote sensing in different fields, such as mapping land cover types and terrain analysis. Hence, Landsat TM (Thematic Matter) thermal bands have proved useful for mapping depositional environments in the Ardakan playa in Iran (Alavi Panah *et al*., 2002).

There are many approaches to mapping surface temperature from thermal scanner data (Lillesand and Kiefer, 1994). Techniques for generating thermal maps from the TM thermal data may have the advantages of reducing cost and time in very poorly accessible regions of the Lut Desert. Remote sensing has shown its greatest value where fieldwork was difficult. Therefore, in this study we applied thermal remotely sensed data in the central Lut Desert that is a poorly accessible region.

Solar radiation depends fundamentally upon climate, but the amount of energy entering the soil is affected by other factors such as, a) topography and slope, b) land cover property, and c) vegetation.

The daytime image is dominated by topographic effects which are made by the solar angle (sun elevation angle) that light reflects on the surface, on the daytime images of the yardang area, and that the ridges and slopes that face South and East are heated more by the morning sun and have bright (warm) signatures in contrast to those facing North.

In desert lands, vegetation cover rarely comes into view, so the land cover property is simply bare soil properties which include moisture content, colour, coarse fragments, texture and structure.

The soil surface temperature is influenced by internal and external factors. The internal factors are thermal conductivity, heat or thermal capacity and thermal Inertia. Thermal conductivity of soil depends on soil physical properties such as soil particles, air, moisture content and porosity. Thermal capacity controls oscillations of temperature; water has high thermal capacity and rocks have low thermal capacity, so water will vary little in temperature between day and night while rocks will vary greatly. Thermal inertia is often dependent on material density; and often increases linearly with increasing material density (Jensen, 2003).

The external factors which influence the surface temperature are meteorological conditions such as solar radiation, air temperature, relative humidity, wind speed, and cloudiness.

Unfortunately, the relationship between true kinetic temperature (internal or true heat) and radiant flux is not perfect. The remote measurement of radiant temperature is always somewhat less than true kinetic temperature. This is due to a thermal property called emissivity (Jensen, 2003). Hince, emissivity has a fundamental function in thermal remote sensing. Furthermore, factors influencing emissivity include: a) color-darker objects are better absorbers and emitters of radiant energy, b) Surface roughness-surfaces that are rough compared to the wavelength of the radiation have more surface area for absorbing and emitting radiation, as surface roughness increases, so does emissivity, c) Moisture content- emissivity increases as moisture increases, d) compaction- more compact material, especially soils, have higher emissivities, e) field of view- the FOV or spatial scale at which you view an object will affect emissivity, f) elec-

[DOR: 20.1001.1.16807073.2007.9.4.1.2]

tromagnetic wavelength- emissivity is wavelength dependent, h) viewing angle- as with BRDF1, emissivity can change with the viewing angle.

The interpretation of thermal remote sensing requires the knowledge of land cover types, and surface temperature in order to yield more reliable results. According to the authors' knowledge, not much research on land cover types and surface temperatures have been published on the yardang landform. Kardavani (1970) stated that the Lut Desert is one of the highest surface temperature zones in the world. Alavi Panah (2003) stated that for a more careful and detailed interpretation of surface temperature of the study area, knowledge on landform and land cover types of yardang is helpful.

In this study, thermal remote sensing analysis was applied to study the surface temperature of desert features and land-cover types of the Lut Desert in the south eastern part of Iran. We attempted to study land the surface temperature of yardang regions in the Lut Desert (Iran) based on field measurements and thermal bands. Due to the hard climatic conditions of yardang region in the Lut Desert, Iran, much information about land surface temperature of this region as one of the most severe climatic condition of the world was not extracted.

The main purposes in this study are: 1) to extract and estimate surface temperature of the Lut desert and 2) to evaluate the efficiency of TM thermal data in the study of surface conditions in desert regions. Therefore, the yardang areas in the Lut Desert, the most severe and hottest temperature zone in Iran, were selected.

STUDY AREA

The Lut Desert is one of the largest playas in Iran and includes a great diversity of hydro-aeolian processes with a very interesting pattern of yardang landforms. Yardangs occupy most part of the western of the central Lut. Terminologically, 'yardang' is used in geomorphology for wind-abraded ridges of cohesive materials (Heiden, 1903; McCauley *et al*., 1970; Cook *et al*., 1993). The total area of the Lut Desert is about 80,000 square kilometers; it is divided into three parts: northern, central, and southern. The study area is located in the central Lut

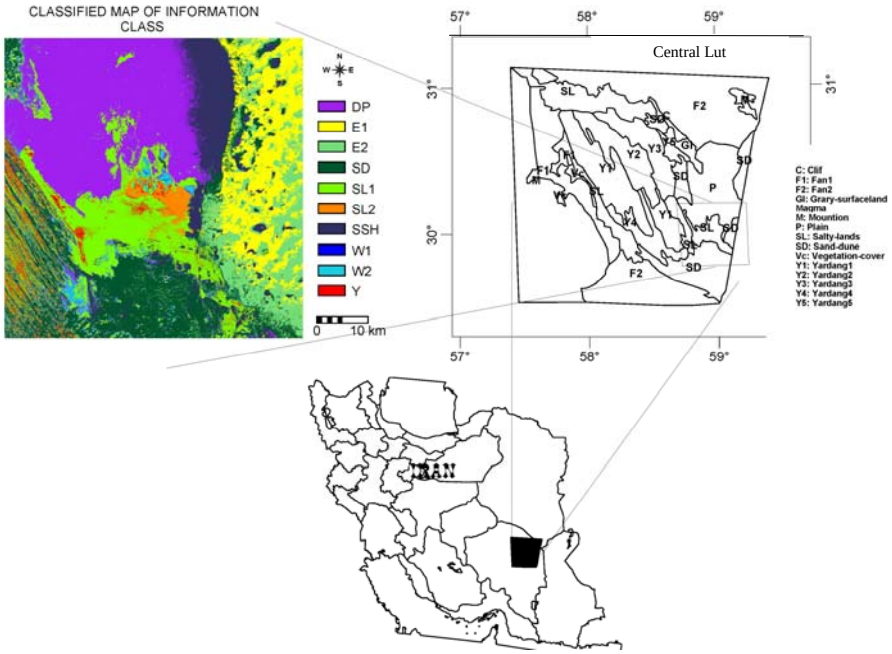

Figure 1. Position of the study area.

[DOR: 20.1001.1.16807073.2007.9.4.1.2]

Desert between 29° 18' 23.14"N, 58° 09' 58 22"E, and 31° 17' 26 82"N, 59° 45' 51.60" E (Figure 1), and it covers about 25, 439 square Km. The Lut Desert, particularly the yardang regions, is characterized by an extremely arid climate with excessive summer heat and an annual rainfall less than 50 mm. The Lut Desert has elevations varying from 4000 m MSL in the Kerman Mountains and 56 m MSL in the yardang regions. The highest part of the yardang regions is 399 m MSL (Bobek, 1969; Mashhadi *et al*., 2003).

Most yardangs occur in unidirectional forms. This optimal form of yardangs minimizes the effect of wind on separation (Kinsley, 1970; Ward *et al*., 1984; Cooke *et al*., 1993).

In general, the study area is characterized by a wide range of land surface characteristics and erosion forms that influence the spectral response. Alavi Panah (2002) has shown that some parts of the yardangs contain a great amount of gypsum and salts.

The study area includes two main regions of yardang and sand dune which are extraordinary and striking features. The southeastern and eastern yardang regions consist of large desert pavements and desert pavements, sand dunes, and salt affected wetlands. Sand regions in the east of the Lut Desert form the largest body of sand in Iran with probably the greatest diversity to be found which is covered with longitudinal crescent dunes.

MATERIALS AND METHODS

In this research, the methodology comprised: 1) field measurements, 2) the relationship between the temperatures in different soil surface and land cover types, 3) diurnal temperature variations in land cover types, 4) primary image processing and fieldwork, 5) image processing, 6) calibration, and 7) the overlay and cross operation of maps and assessment (Figure 3). In this study, the air conditions and surface temperature of the important features such as marl, grey sand, bright sand ,surface soil and subsoil (at a depth of 10 centimeters) and salt affected land was measured by thermometer eight times a day from 6 a.m. to 8 p.m. during a 15-day period. The correlation coefficient between the air temperature, and the other measurements was calculated (Ta-

Figure 2. Some important land cover types of the yardang region in the Lut Desert.

[DOR: 20.1001.1.16807073.2007.9.4.1.2]

Table 1. The descriptive information of classes in the study area, Lut Desert.

Type	Code	Area (Km^2)	Description
Yardangs	*Y*	104.39	Ridged remnant rounded hills with silty-loam texture and hardly cemented
Huge pyramids dunes (Erg)	*E1*	417.62	Huge pyramid dunes in southeastern part of Lut
	E2	361.34	Local drainage within huge pyramid dunes with low reflectance and high moisture
Sand dune	*SD*	556.17	Sand dunes in the eastern part of near yardangs with branches and silk
Sand sheet	*SSH*	320.30	Sand sheet in the western of huge pyramid dunes
Desert pavement (Rig)	*DP*	923.33	Desert pavement with rig levels in the Lut Plain, between yardangs and huge pyramid dune
Salty lands	*SL 1*	541.26	Salty-covered land with high reflectance
	SL 2	50.65	Salty land with lower salt content than above with wind and water erosion
Low wetland	*W1*	1.64	Low wetland and the end of drainage with high-level underground water
	W2	124.30	The moisture content is relatively lower than the above

ble 1), then the relationships between them was investigated by least square fitting (LSF) function and the linear and polynomial models were fitted between them (Figure 4). In addition to field measurements, Landsat satellite TM thermal dated from 25 June 1989 and other sources of data and maps were used. In order to calculate land surface temperature and further image processing, a window in the southeast of the yardangs (with 1,960 columns and 2,028 pixels) was selected (Figure 1). In this study, we hypothesized that Landsat TM data with a spatial resolution of 30 m for reflective bands and 120 m for the thermal band are useful to study land cover types and surface conditions. Therefore, TM 6 data as a representative of surface temperature is used to display the variation of thermal data. In addition to Landsat TM data, other information sources, such as topographic maps (1: 50,000), geologic maps (1: 250,000), and aerial photos (1: 20,000) were used. Upon the window in the southeast of the yardangs (1,960 columns and 2,028 pixels) was used to classify by image processing In addition, land cover types were defined by field observations, the training sets were identified, and spectral patterns of different types of land covers were generated. Based on the results obtained from OIF, TM bands 1, 4, 5, 7 as the most informative TM reflective bands were used to classify land cover types using the pixel maximum likelihood classification algorithm (Figure 3). For the sample set and training area, 10 different information classes were distinguished in which one class is related to yardangs (Table 1). Prior to applying thermal detection analysis, image processing operations were performed on the remotely sensed data in order to identify environmental conditions and content features. The fieldwork as one of the most important steps was carried out in autumn 2000 to confirm the nature of the findings in which the land cover types were defined correctly, and the training sets were identified well. The class separability analysis was carried out by computing the statistics (mean and standard deviations) in which according to the obtained results of OIF, the most informative TM bands were selected and then

[DOR: 20.1001.1.16807073.2007.9.4.1.2]

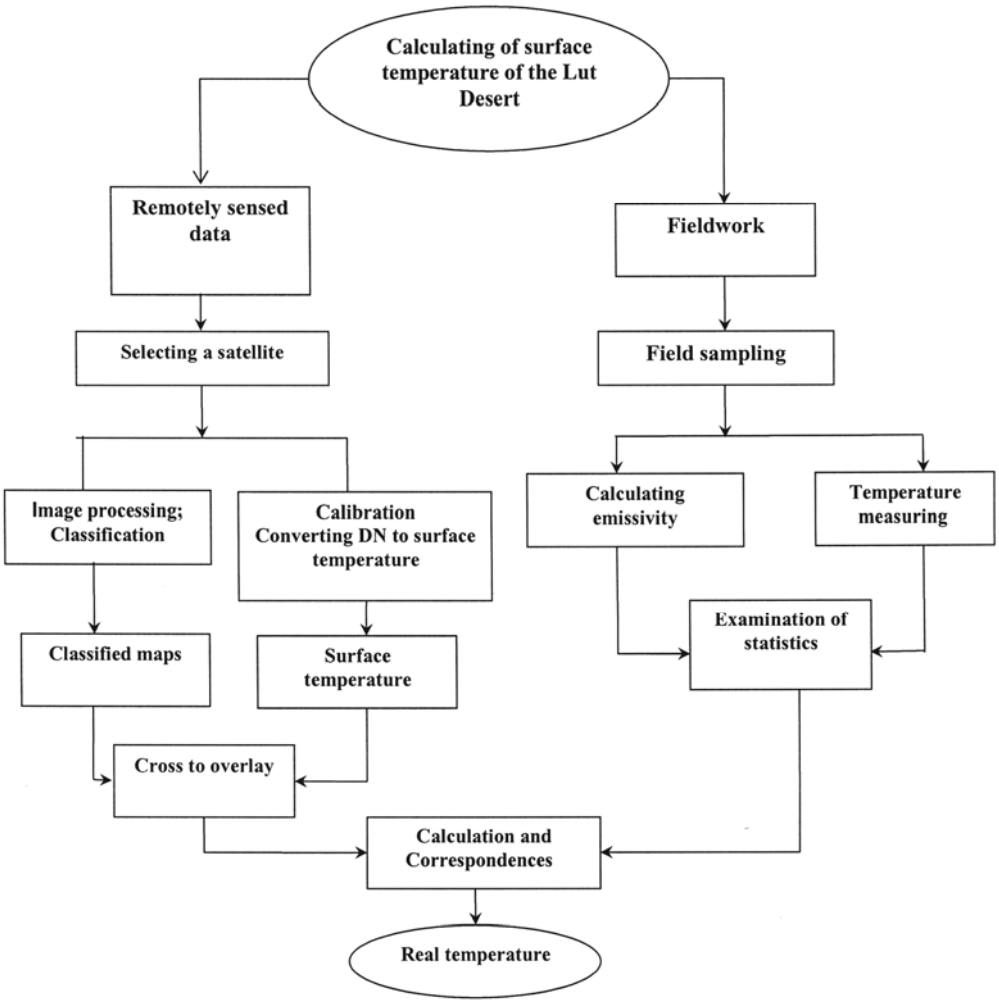

Figure 3. Flowchart of the methodology in the study.

all data sets were classified using the pixel maximum likelihood classification algorithm and finally the land cover map was produced. The most important procedures in the preprocessing are radiometric calibration, followed by then the calculating of thermal conversion. Hence, just the thermal band of the TM sensors was included in the processing and further analyzing. This band was individually subject to calibration and calculation. This process included the conversions of digital number (DN) values to at-satellite radiance values (Markham and Becker, 1986).

$$L\lambda = \left\{\left(\frac{(Lmax - Lmin)}{255}\right) \times DN\right\} + Lmin \quad (1$$

Where:

$L\lambda$ = Spectral radiance in $W.m^{-2}.ster^{-1}.mm^{-1}$

L max= Maximum spectral radiance in $W.m^{-2}ster^{-1}.mm^{-1}$ (at DN=255)

L min= Minimum spectral radiance in $W.m^{-2}.ster^{-1}.mm^{-1}$ (at DN=255)

The brightness surface temperature of the land surface (T_B) is the kinetic temperature of the soil plus the canopy surface (or, in the absence of vegetation, the temperature of the soil surface). A blackbody having a kinetic or surface temperature (temperature meas-

[DOR: 20.1001.1.16807073.2007.9.4.1.2]

ured by a thermometer inside the body) emits a wavelength energy that responds to Planck's law (Chemin, 2002).

In the thermal range, the relation between black and grey bodies is simplified by a property called emissivity (a blackbody has an emissivity equal to one and it is independent of the wavelength). In the case of natural bodies, the thermal emission depends on the emissivity, which is also variable for different wavelengths. A remote sensor works within a spectral range, coinciding with an atmospheric window. It only reads a portion of the body radiation. If the emissivity is known, the real surface temperature can be obtained by inverting the Planck equation for real bodies (Chemin, 2002).

The calculation of brightness surface temperature using this sensor is particularly designed, because of some thermal band sensor drift. The black body radiation emitted at a spectral width of band 6, $L\lambda$, at the top of atmosphere image can be processed following the inverse Planck function based on the outgoing spectral radiance of the band 6 at the earth brightness surface (Markham *et al*.,1986):

$$T_B = \frac{K_2}{\ln\left(\frac{K_1}{L\lambda}+1\right)} \quad (2$$

Where $L\lambda$ is the blackbody spectral radiance in $W.m^{-2}.ster^{-1}.mm^{-1}$, T_B is brightness temperature integrated over the TM band 6 in degrees Kelvin, and *K1* and *K2* are two free parameters (constant) with the values of *K1*= 607.76 $W.m^{-2}.ster^{-1}.\mu m^{-1}$ and *K2* = 1260.56 Kelvin. In spite of the deficiency of *in situ* or ground measured information of the weather conditions at the time of satellite data acquisition, therefore, atmospheric correction is deemed unnecessary for the image in deserts, since there are clear skies, low humidity levels and the temperature values area derived from the image are almost equal to *in situ* temperature values (Lillian *et al*., 2005). In addition, Weng (2004) stat that the horizontal variation could have been minimized by using an image acquired in a highly clear day and covering a small area. Errors due to urban effective anisotropy depend upon surface structure and relative sensor position, and can yield a temperature difference of up to 6 K or higher in downtown areas, despite, the calibration of Landsat TM6 radiometrically corrected by using minimum and maximum spectral radiance (instead of gain and offset), in addition. After that, supervised classification methods were applied to classify the TM multispectral image to land-cover map and to derive associated surface emissivity and, then, a cross operation was performed to overlay two maps (classified map and thermal map). Pixels on the same positions in both maps are compared; the result has been aggregated in Table 5.

The fieldwork, as one of the most important steps, was carried out in October, 2000. Visual image interpretation was used to identify the land cover types of the area. The standard TM color composite to the scale of 1: 100,000 and aerial photos to the scales of 1: 50,000 were the main images and maps used in the field. Some other maps, such as topographic and geologic maps were used during the fieldwork for delineating the boundaries of the morphologic units and land cover types. As a result, the classes of yardang (Y), desert pavement (DP), sand dune (SD), great sand dunes (Erg 1 and Erg 2), salty land (SL 1 and SL 2), and wetland (W1 and W2) were trained (Table 1).

Purposive samplings are carried out where typical sites are chosen for a special goal. Proponents of purposive sampling argue that the resultant samples are very representative since they are based on the skills and the local knowledge of the field worker. Based on the results obtained from the fieldwork and the information obtained from the maps (1: 50,000), aerial photos (1: 20,000), geologic maps and our personal experience in Iran deserts, gained over 20 years the training areas were chosen to classify the TM images. After land cover classification by selecting training areas on false color composite images in association with a 1:50000 topography map, the study area was classified in a total of 10 information classes (Ta-

[DOR: 20.1001.1.16807073.2007.9.4.1.2]

Table 2. The average of temperature in 15 days in Celsius (º C); H represents hours from 6 a.m. till 8 p.m.

	H6	H8	H10	H12	H14	H16	H18	H20
Soil Depth (10 cm)	32.3	35.6	43.5	52.0	50.7	48.1	44.1	41.5
Dry Air	30.3	32.3	35.2	38.3	40.0	41.4	40.8	40.0
Gray Sand	30.1	33.5	40.5	47.9	50.1	50.8	47.4	44.6
Marl	30.6	34.5	41.9	50.7	51.9	51.8	46.9	44.3
Light Sand	30.5	33.6	39.6	47.8	50.3	52.3	48.2	45.8
Shadow	30.1	32.2	35.2	38.6	40.0	41.4	40.8	39.7
Surface Soil	31.0	35.8	44.1	50.7	50.5	48.5	43.9	41.6
Wet Air	15.3	15.7	17.1	18.5	19.2	19.4	19.3	18.5

Table 3. The result of estimation of power function (Y= the function of feature, X= Relation to dry air) and R-square; Y = a×exp (b × x), where X (variable = Dry air temperature) and Y (other feature temperature) are known variables and where *a* and *b* are unknown coefficients.

Feature	$Y = aX^b = a \times pow(X, b)$	R^2
Grey sand	Y = 0.1265×pow(X, 1.6097)	0.9408
Light sand	Y = 0.1051×pow(X, 1.6633)	0.9638
Marl	Y = 0.1501×pow(X, 1.5685)	0.8782
Soil surface	Y = 0.4697×pow(X, 1.2484)	0.7153
The depth of soil(10 cm)	Y = 0.5991×pow(X, 1.1826)	0.6898

bles 5 and 6) such as yardangs, desert pavements, salty lands (two classes), sand sheets, sand dunes, great Ghourds (two classes) and wetlands (two classes). Table 1 shows the descriptive properties of the information classes of the Lut Desert.

We also collected ground information and surface temperature by field sampling from 28 August to 18 September in 2000 (Table 2). Ground information was collected over four physical features of different land cover types. The two-hourly surface temperatures (*TG*) observed on the ground field sampling at the time of the Landsat-5 overpass and every two hours by thermometer.

RESULTS

Surface temperatures

The location of sites where field sampling was done and considered sufficiently homogenous, the results after statistical operations such as calculating the average of numbers, calculating the least squares fit through inter points by using the equation for every variable (Figure 4 and Table 3), and the least squares fit operation calculation for all discrete values (in ILWIS) in two input columns (dry air and other features) to find the relation of the temperature of every feature with dry air temperature, resulted in an output (predict) value that was calculated on best function to study and determine the relationship of functions of variables. Thus, the least squares fit operation provided the best fitting relation between dry air and other features; the best fit between the dry air temperature and other temperature features was calculated by using an exponential function (always 2 terms) defined by the line (Figure 4 and Table 3).

Regarding the statistical model in Figure 4, this shows how the temperature of features (sand, soil, etc.) correspond with the air dry

[DOR: 20.1001.1.16807073.2007.9.4.1.2]

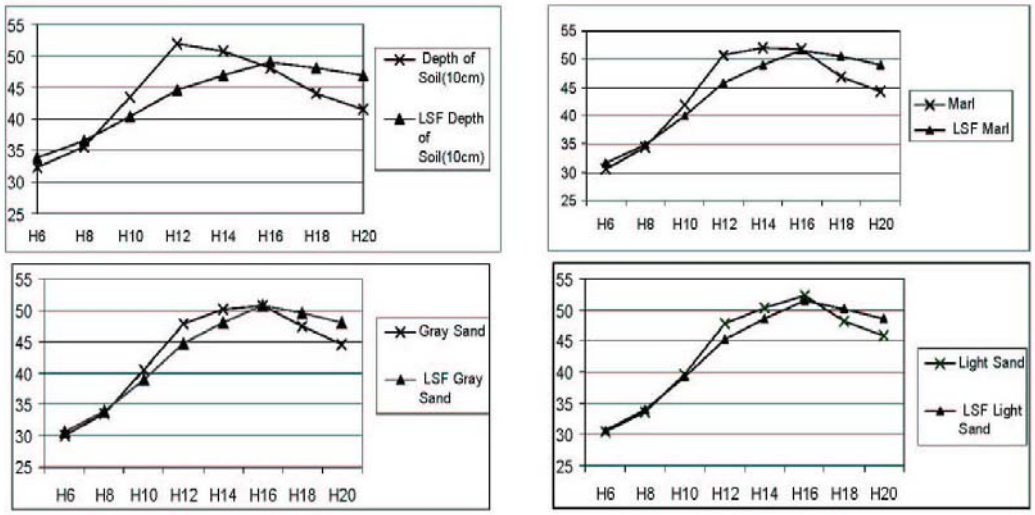

Figure 4. The comparison of real temperature and estimated temperature according to Least Square Fitting (LSF),Y-axis presents temperature in Celsius (º C)and X-axis also presents times in every two hours during a day between 6 a.m. until 8 p.m..

temperature, therefore, due to the low thermal capacity of sand, the R^2 value grows to be higher than 0.94, despite the fact that the R^2 value of features such as marl, surface soil, and the 10-centimetre depth of soil decreased respectively. So it is related to the thermal capacity in marl and surface soil, however, in addition to the factor, at the 10-centimetre depth of soil temperature, the thermal diffusion coefficient is involved and causes the minimum R^2 and instability of the model. Another fault in the model for estimating temperature is that it shows a higher temperature than the real temperature before maximum level (peak) and a lower temperature after it.

Thermal Infrared Environmental Considerations

The typical diurnal temperature variations for soil and marl sand are shown in Figure 5. If all of these curves lay exactly on top of one another, then remote sensing in the thermal infrared portion would be of no value because all the phenomena would have the same apparent radiant temperature. There would be no contrast in the imagery between the different phenomena. Fortunately, there are two times during the day (after sunrise and near sunset) when there is some radiant temperature. During this crossover time period it is generally not wise to acquire thermal remotely sensed data. Opportunely, some materials store heat more efficiently than others, i.e. they have a higher thermal capacity than soil and sand. For example water has a higher thermal capacity than soil; its diurnal temperature range fluctuates very little when compared with the dramatic temperature fluctuation of soil and sand during a 24-hour period.

If we were interested in performing temperature mapping of terrain consisting just of soil sand and marl, we could predict what the image would look like if we acquired it at about 9.30 a.m.-2 p.m.. and at 4 p.m. The soil would appear brighter than sand in the morning thermal imagery due to their high apparent temperature.

In the early evening, sand and marl are still warmer than soil. Because salt affected

[DOR: 20.1001.1.16807073.2007.9.4.1.2]

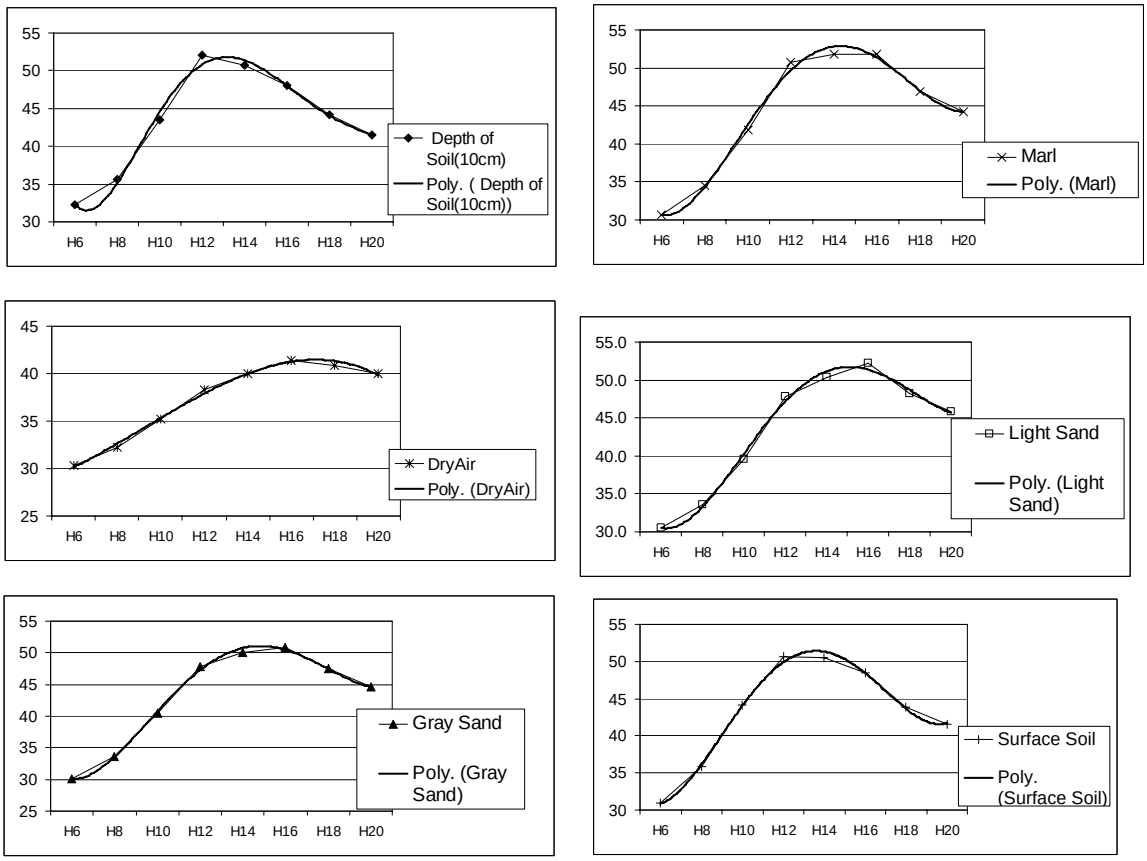

Figure 5. Diurnal temperature of studied variables and polynomial graph of average of temperature; Y-axis presents temperature in Celsius (ºC) and X-axis also presents times in every two hours during a day between 6 a.m. until 8 p.m..

vegetation contains water, it is usually cooler (darker) than sand and marl on daytime imagery and warmer (brighter) than sand on predawn imagery. It is apparent that the diurnal variation of soil temperature is considerable, even at the lower depths where it is not affected by air temperature (Baybordi, 1987). As Figure 5 shows, the surface layer temperature varies more or less according to the air temperature and, in places where surfaces exhibit a solar control and a clear sky, the temperature of the surface layer increases as long as air temperature rises from morning reaching a maximum at about 2 to 6 p.m.

If we were interested in temperature mapping of terrain consisting of just soil, rock, and water, we could predict what the image would look like if we acquired thermal infrared imagery at about 2 p.m. and 4 a.m.. The soil and water appear brighter than water in daytime thermal imagery due to their higher apparent temperature. Rock and soil continue to radiate (emit) energy into the atmosphere during the night. During the early evening, rock and soil are still warmer than much of the surrounding terrain. Based on the results obtained from the ATLAS mission that was flown over a large sandbar in the Mississippi River at 5 a.m. and 10.30 a.m., the data have a spatial resolution of 2.5×2.5 m. Daytime thermal bands 10, 11, 12 reveal a dramatic difference in the temperature properties of sand and gravel on the sandbar. The different materials absorb the incidental energy from the sun differently,

[DOR: 20.1001.1.16807073.2007.9.4.1.2]

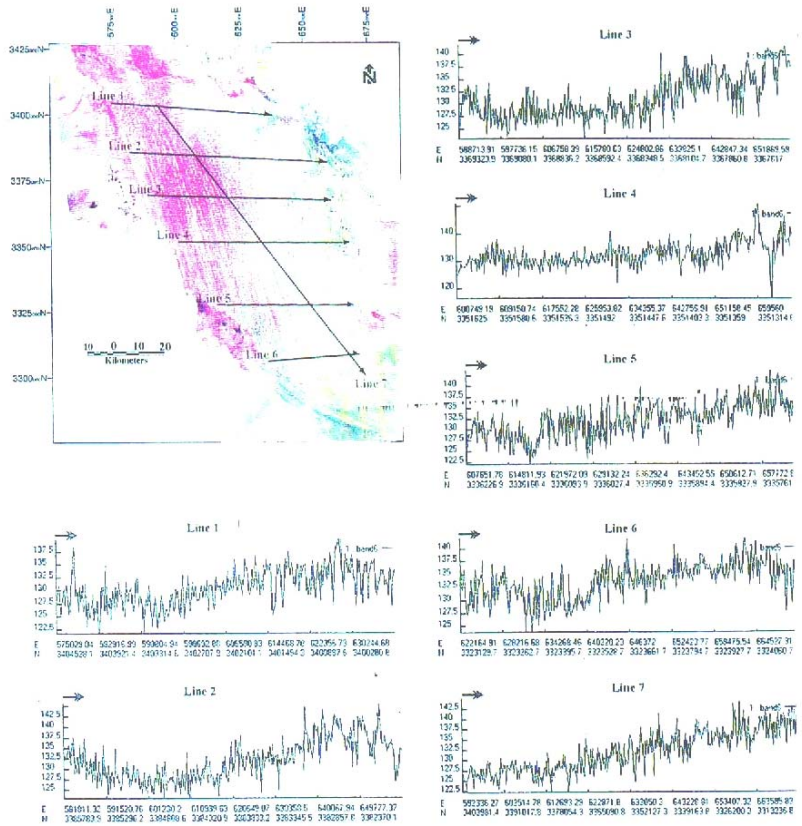

Figure 6. Thermal DN value information along six specified transects from West to East (lines 1 to 6). line 7 shows the thermal DN values from Northwest to Southeast.

resulting in substantial differences in appearance from the sand and gravel surfaces in the three thermal infrared bands. According to Table 3, we can estimate the temperature of each feature base on proposed functions; Table 4 presents the results of estimated temperature in this way. Also, Figure 4 displays how the estimated results fit to real temperature.

Variation of Thermal Values

The TM band 6 data of the yardang region shows that the data lie in a narrow range of 69 to 176 out of a total range of zero to 255. Figure 6 shows the stretched TM thermal image of yardang with seven transects on it. DN values along the transacts (lines 1 to 6) suggest that a zone of relatively higher thermal values could be delineated in the eastern part of the yardang when compared with the values present in the western and middle part. This difference in thermal values (as a surrogate of surface temperature) suggests that this kind of lineament has acted as a thermally different zone divider.

These observed thermally different zones might be related to the material types and surface moisture contents. Line 7 in Figure 6, shows the trend of thermal DN values from the northeast to southwest. Figure 6, shows transects 1 to 6 with various peaks and valleys which may correspond to the ridges and furrows with different surface

[DOR: 20.1001.1.16807073.2007.9.4.1.2]

Table 4. Result of estimation according to power function (Least Square Fitting).

Hours (H)	Grey Sand	Light Sand	Marl	Soil surface	The Depth of Soil (10 cm)
6	30.7	30.6	31.6	32.2	33.8
8	34	34	34.9	36	36.5
10	39	39.3	40	40	40.4
12	44.7	45.2	45.7	44.5	44.7
14	48	48.6	48.9	47	47
16	50.7	51.4	51.6	49	49
18	49.5	50.2	50.4	48.2	48.1
20	48	48.6	48.9	47	47

materials, topographic conditions, shadows and sunlight illumination.

The peak with the highest TM digital numbers is mainly associated with sun-exposed ridges, sand sheets or sand dunes. The valleys correspond to shadows and other phenomena with a low temperature. The fourth transect shows that a deep valley exists near the endpoint of line 4 which represents the wet zone.

A color printout image of the Landsat TM in 1990 was used during the fieldwork (Figure1). Descriptive information, which includes identification and spreading of bare soil and sand dunes, was noted for each site. These records were compared to the soil type and land cover and then used as reference and validation information for satellite image processing. Figure 8 presents the results of thermal detection superimposed on the surface temperature values of Band 6 in 1989 as grey-levels. Brighter tones in the background indicate higher surface temperature values while darker tones indicate lower ones. Temperature is highlighted in colors ranging from blue to red. A high temperature is colored red and a low temperature changes to blue.

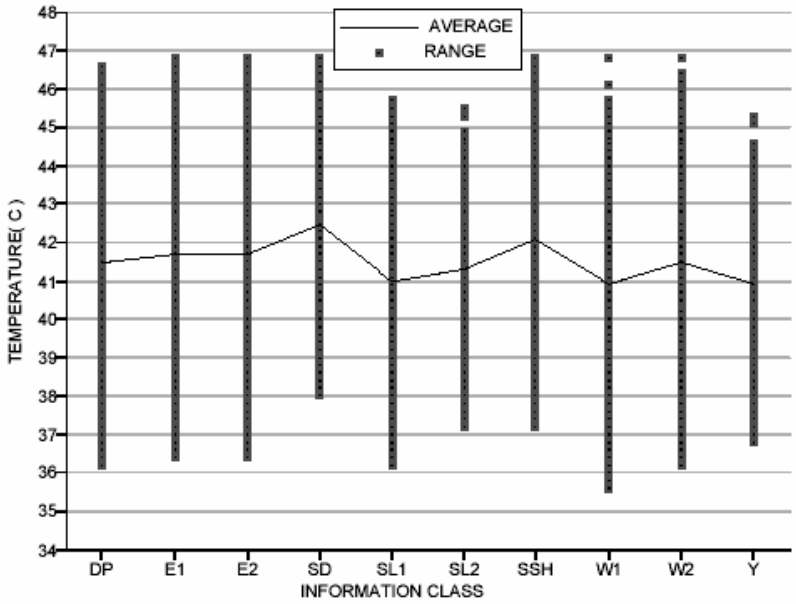

Figure 7. The result of overlaying two maps (classified map and thermal map) and the variation of temperature among the classes in the study in Celsius (ºC).

[DOR: 20.1001.1.16807073.2007.9.4.1.2]

Figure 9 also presents three cross-sections that show temperature values along the distance. The graph shows that the first point of line 2 lies in a yardang while the end of the cross-section is in a relatively flat salty area 25 Km away. The temperature drops, respectively, in regions such as wetlands, salty lands, desert pavement, and yardangs but it increases in sandy regions.

The graph in Figure 10 also displays the results such as maximums, minimums, and averages of temperature in information classes, according to the results the average temperature of E1 is the highest class and W1 is the lowest class. The maximum and minimum sand dune temperature (SD) is the highest class and W1 is the lowest class which is statistically provided in Table 5. The result shows the role of thermal capacity of features.

CONCLUSION

This study has demonstrated the utility of TM data for mapping the Lut Desert features including yardangs, sand dunes and some other land cover types with relatively high spatial resolution satellite data. We concluded that Lut Desert land cover types, such as yardangs, and sand dunes and salty lands, carry unique and important information about the desert's characteristics. This study also showed that, in some cases, only a slight spectral difference could be used effectively in the discrimination of desert land cover types on the basis of their spectral signatures. Based on results obtained from field observations, we may generally conclude that non-aeolian processes such as cracking, piping, riling and salt weathering are very important in developing and forming yardangs. To achieve high classification accuracy, extensive fieldwork and aerial photos are very effective. The result of visual interpretation of various band combinations may improve our knowledge of the spectral reflectance of wetlands, sand dunes and yardangs and, therefore, it may provide an opportunity for delineating land cover units.

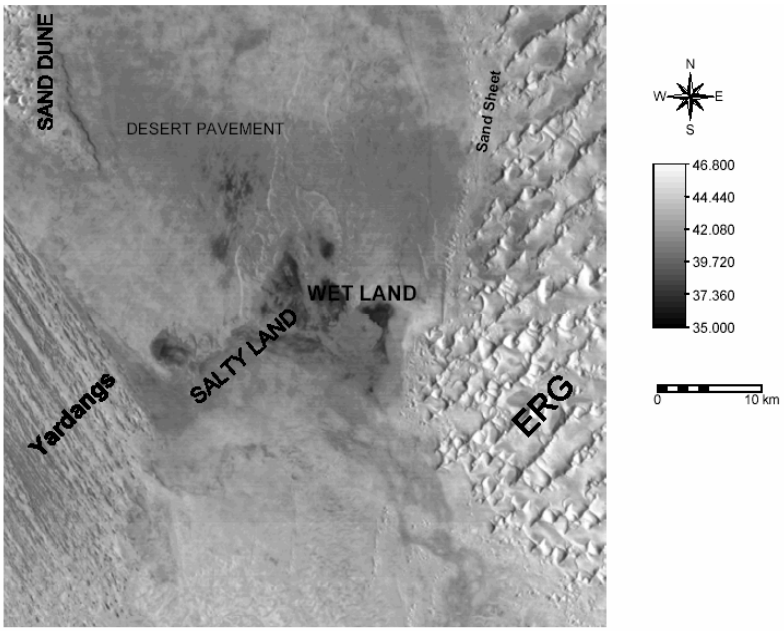

Figure 8. Surface temperature distribution in the Lut Desert derived from the TM band 6 image data the variation of temperature is in Celsius (° C).

[DOR: 20.1001.1.16807073.2007.9.4.1.2]

Table 5. The result of overlaying two maps (classified map and thermal map), the dimension is temperature in Celsius (º C).

Type	Code	Average (º C)	Minimum (º C)	Maximum (º C)	Range (º C)
Desert pavement	DP	41.47	36.20	46.60	10.40
Great sand dune Erg	E2	41.67	36.40	46.80	10.40
	E1	41.67	36.40	46.80	10.40
Salty lands	SL2	41.30	37.20	45.50	8.30
	SL1	41.00	36.20	45.70	9.50
Sand sheet	SSH	42.44	38.00	46.80	8.80
Low-level wet lands	W1	40.91	35.60	46.80	11.20
	W2	41.48	36.20	46.80	10.60
Yardangs	Y	40.93	36.80	45.30	8.50

Based on the results obtained from calibration we may conclude that hyper-arid climatic conditions are ideal conditions for mapping detailed land cover types and understanding the behavior of TM thermal and TM reflective bands. The results obtained from fieldwork have revealed that wind and water do not work in isolation; quite on the contrary, they work in close partnership.

These further researches appear to be necessary for improving our knowledge about mapping surface temperatures based on satellite thermal data. We may also conclude that Landsat data can be applied for mapping yardang land cover types. The digital images are available with a worldwide coverage for different seasons and over a period of many years.

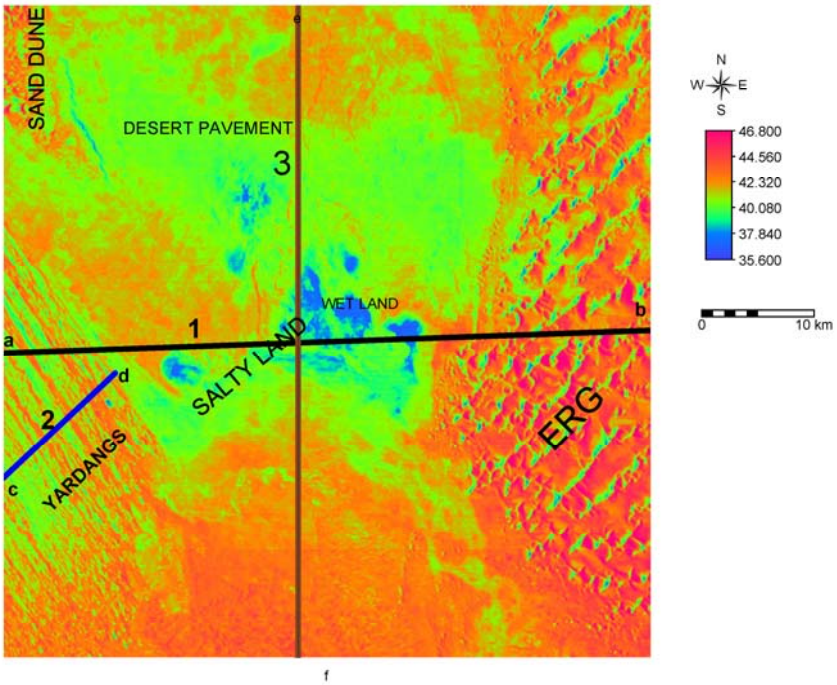

Figure 9. Highlighted surface temperature distribution in the Lut Desert derived from the TM band 6 image data and cross-section.

[DOR: 20.1001.1.16807073.2007.9.4.1.2]

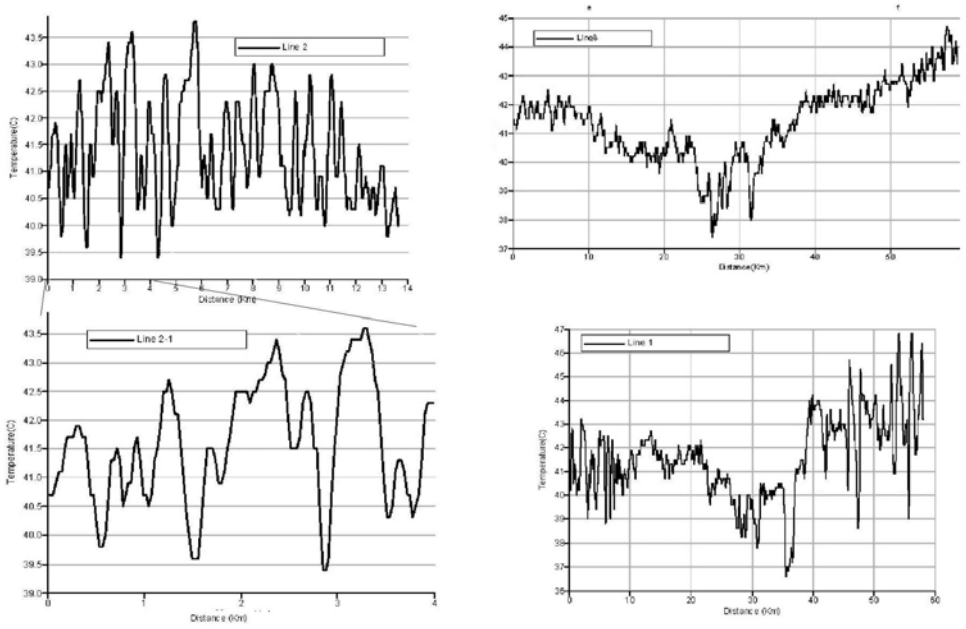

Figure 10. Three cross-sections over study area that shows the variation of surface temperature, in which the Y-axis presents temperature in Celsius (º C) and the X-axis also presents distance in Km.

Global availability of aerial photographs is limited, therefore such availability of satellite data allows the images to be selected at optimal times for land cover change detection. We expect that the method of extraction of surface temperature based on remotely sensing data will be used in desert areas.

ACKNOWLEDGEMENTS

The current research presented in this paper was carried out within the framework of a project which was supported by the Vice Chancellor for Research, University of Tehran. We would also like to express our thanks to the Iranian Remote Sensing Center for providing the Landsat TM data.

REFERENCES

1. Alavi Panah, S. K. 2003. Study of Surface Temperature the Lut Desert Based upon Landsat Thermal Band and Field Measurement, *Biaban*, **7 (2)**: 67-79.
2. Alavi Panah, S. K. 1997. Study of Soil Salinity in the Ardakan Area, Iran, Based upon Field Observations, Remote Sensing and GIS. Ph. D. Thesis. University of Gent 292pp.
3. Alavi Panah, S. K., Barzegar, F., Ahmadi, H., and Komaki, Sh. B. 2002, Study of Yardangs of Lut Desert Based on Image Processing, Academic Research, University of Tehran, 150 pp.
4. Alavi Panah, S. K., De Dapper, M., Goossenes, R., and Masoudi, M. 2001. The Use of Thermal Band for Land Cover/Land Use Mapping in Two Different Environmental Conditions of Iran. *J. Agri. Sci. Agric. Sci. Techno*l. **3**: 27 -36.
5. Alavi Panah, S. K., Sarajian, M. R. and Komaki, Sh. B. 2002. Temperature Map of Lut Desert Using Thermal Band of Landsat Satellite. *Biaban*, **7 (1)**: 85-99.
6. Baybordi, M. 1987. *Soil Physics*, Tehran University Publication, no. 1672, 523 pp.
7. Bobek, H. 1969. *Zur Kennis der sudlichen Lut. Mittlungen der Ostereicher*

[DOR: 20.1001.1.16807073.2007.9.4.1.2]

geograpischen Gesselschaft, Wein 3, 155-192pp.
8. Chemin Y. 2002 "Evapotranspiration by Energy Balance Budget, Applied Theory to Common Satellite Sensors" PhD Special Study Report, Asian Institute of Technology, Bangkok, Thailand, March, 25pp.
9. Cooke, R. U., Warren, A. and Goudie, A. S. 1993. *Desert Geomorphology*, University College London Press, London.
10. Drake, N. A. 1995. Reflectance Spectra of Evaporate Minerals; Applications for Remote Sensing. *Int. J. Remote Sens*., **16(14)**: 2555-2571.
11. Ehsani, A. H., and Alavi Panah, S. K. 2002. Study of the Damghan Playa Margin Based upon Landsat Satellite ETM+ Bands. *Proc. Sympos. Geomatics*, 22-25 April, 2002, Tehran, Iran.
12. Heiden, S. 1903. *Central Asia and Tibet* (2volume). New York: Scribners.
13. Kardavani, P. 1970. *Some Soil Samples of Shahdad Area (Kerman) No.5*. Institute of Geography, University of Tehran.
14. Krinsley, D. H. 1970. A *Geomorphologic and Poleoclimatogic Study of the Playas of Iran*. USGS, Final Scientific Report. (Contract PROCP 70-800), US Airforce Cambridge Research.
15. Li, Z. L., and Becker, F. 1993. Feasibility of Land Surface Temperature and Emissivity Determination from AVHRR Data. *Remote Sens. Envir*, **43**: 67-85.
16. Lillesand, T. M., and Kiefer, R. W. 1994. *Remote Sensing and Image Interpretation*, (4th Edition) John Wiley and Sons, New York,
17. Wang, L. T., and De Liberty, T. L. 2005. Landsat Atmospheric Correction : The Good, the Bad, and the Ugly, *2005 ESRI International User Conference Proc*. gis.esri.com/ library/userconf/proc05/papers/ pap1560.pdf
18. Mashhadi, N., Alavi Panah, S. K. and Ahmadi, H. 2003. Geomorphology Studies of Lut Yardang. *Biaban*, **7(2)**: 25-43
19. Markham, B. L., and Becker, J. L. 1986. Landsat MSS and TM Post-calibration Dynamic Ranges, Exoatmospheric Reflectances and At-satellite Temperatures, *EOSAT Landsat Tech. Notes*, **1**: 3-7.
20. MC Cauley, J. F., Grolier, M. J. and Breed, C. S. 1970. Yardangs of Peru and Other Desert Regions. *USGS Interagency Report, Astrogeology* 81.
21. Norman, J. M., Divakarla M. and Goel, S. 1995. Algorithms for Extracting Information from Thermal _ IR Observations of the Earth's Surface. *Remote Sensing Environment*, **51**: 157-168.
22. Ward, A. W. and Greeley, 1984. Evaluation of the Yardangs at Rogers Lake California. *Geological Society of America, Bulletin*, **95**: 829-37.
23. Weng, Q., Lu, D. and J. Schubring. 2004. Estimation of Land Surface Temperature-Vegetation Abundance Relationship for Urban Heat Island Studies. *Remote Sensing of Environment*, **89(4)**: 467-483.

[DOR: 20.1001.1.16807073.2007.9.4.1.2]

دمای سطح یاردانگ‌های بیابان لوت بر اساس انگیری‌های میدانی و داده‌های حرارتی ماهواره

س. ک. علوی پناه ، م. سراجیان، غ. ر. ثواقبی، چ. ب. کمکی، ا. مقیمی و م. کریم پور ریحان

چکیده

به دلیل شرایط سخت حاکم بر یاردانگ‌های بیابان لوت (ایران)، اطلاعات زیادی پیرامون دمای سطحی این منطقه به عنوان یکی از سخت‌ترین شرایط اقلیمی جهان، به دست نیامده است. بنابراین در این مطالعه، برای اینکه اطلاعاتی پیرامون پدیده‌های سطحی بیابان لوت (مارن، ماسه خاکستری ماسه روشن و زمین‌های شور به دست آید از روش اندازه‌گیری دما در منطقه مورد مطالعه و پردازش داده‌های سنجش از دور استفاده شد. دمای سطوح مورد مطالعه در ۸ نوبت از ۶ صبح تا ۸ بعد از ظهر به مدت ۱۵ روز در اکتبر سال ۲۰۰۰ اندازه‌گیری شد. علاوه بر اندازه‌گیری میدانی از داده های حرارتی TM ماهواره لندست به تاریخ ۲۵ ژوئن ۱۹۸۹ نیز استفاده شد. سپس تجزیه و تحلیل سنجش از دور حرارتی برای تهیه نقشه دمای سطحی در بخش جنوب شرقی بیابان لوت (ایران) به عمل آمد. در این تحقیق، روش های زیر به کار گرفته شد: ۱) اندازه‌گیری میدانی ۲) رابطه بین دمای سطوح خاکهای مختلف و پوشش زمین ۳) تغییرات روزانه دمای سطحی پوشش زمین ۴) پردازش اولیه تصاویر و کالیبراسیون ۶) طبقه‌بندی تصویر و ارزیابی صحت ۷) تهیه نقشه دمای سطحی بر اساس تبدیل تابش سطحی پدیده‌ها. سپس اختلاف معنی‌دار بین دمای سطحی مختلف از ۶ صبح تا ۹ ، مورد بحث قرار گرفت نتایج حاصله اهمیت سنجنده‌های حرارتی از نقطه نظر زمان عبور و یا تصویر برداری نشان داد. بر اساس نتایج حاصل از داده‌های حرارتی و اندازه گیری‌ها، دمای پدیده‌ها به ترتیب از زمین‌های مرطوب، زمین‌های شور، سنگ‌فرشهای بیابانی، یاردانگ و ماسه زار افزایش می یابد.

[DOR: 20.1001.1.16807073.2007.9.4.1.2]